Supporting Information

Unveiling the Impact of Crosslinking Redox-Active Polymers on Their Electrochemical Behavior by 3D Imaging and Statistical Microstructure Analysis

Marten Ademmer [a,§], Po-Hua Su [b,c,§], Lukas Dodell [a], Jakob Asenbauer [b,c], Markus Osenberg [d], André Hilger [d], Jeng-Kuei Chang [e,f], Ingo Manke [d], Matthias Neumann [a,*], Volker Schmidt [a], Dominic Bresser [b,c,*]

[a] *Institute of Stochastics, Ulm University, 89069 Ulm, Germany*

[b] *Helmholtz Institute Ulm (HIU), 89081 Ulm, Germany*

[c] *Karlsruhe Institute of Technology (KIT), P.O. Box 3640, 76021 Karlsruhe, Germany*

[d] *Institute of Applied Materials, Helmholtz-Zentrum für Materialien und Energie, 14109 Berlin, Germany*

[e] *Department of Materials Science and Engineering, National Yang Ming Chiao Tung University, Hsinchu 30010, Taiwan*

[f] *Department of Chemical Engineering, Chung Yuan Christian University, Taoyuan 32023, Taiwan*

Keywords: 3D microstructure characterization; synchrotron X-ray tomography; nano-structured carbon; organic batteries; statistical image analysis

***Corresponding authors:** dominic.bresser@kit.edu; matthias.neumann@uni-ulm.de

[§]These authors contributed equally.

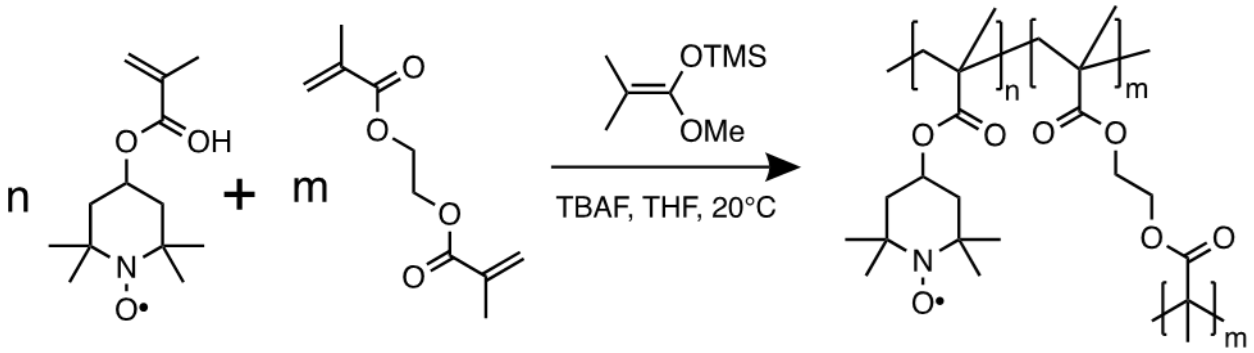

Figure S1. Synthesis scheme for yielding (crosslinked) PTMA with m = 0 for G-PTMA and m $\neq$ 0 for crosslinked XG-PTMA.

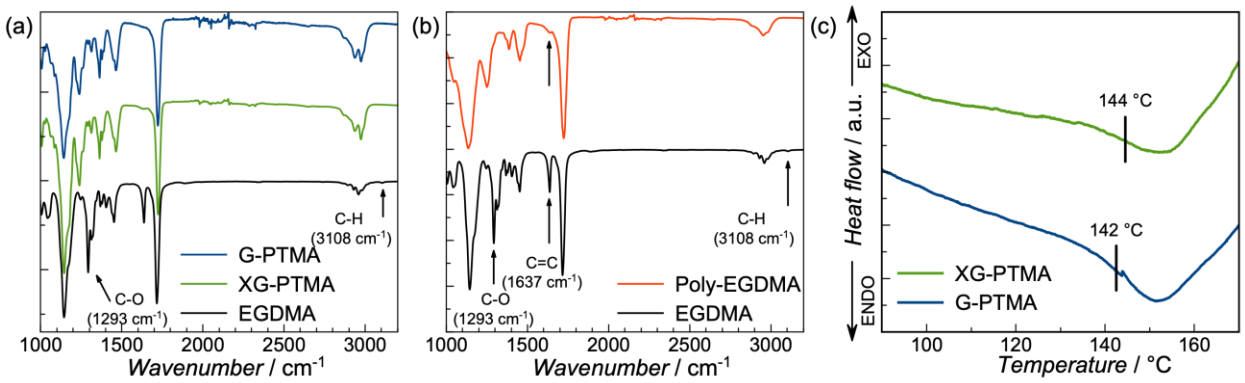

Figure S2. (a) FTIR spectra of G-PTMA (blue), XG-PTMA (green) and the cross-linker, ethylene glycol dimethacrylate (EGDMA; black). (b) Comparison of the FTIR spectra of EGDMA (black) and poly-EGDMA (orange). (c) DSC data recorded for (X)G-PTMA, conducted with a scan rate of 5 □ min^{-1} during the second heating cycle.

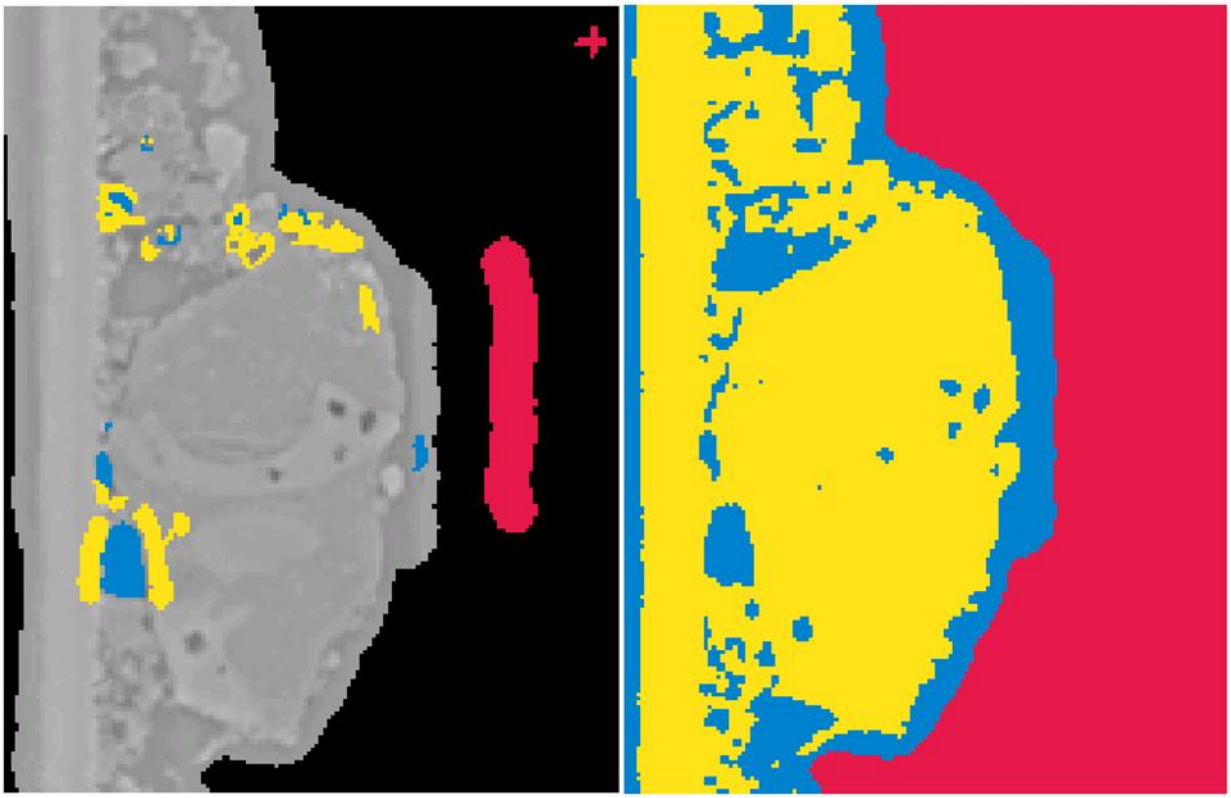

Figure S3. Example cutout of the hand-labeled training data of the sample with G-PTMA-CMK-8 on the left and the same cutout labeled by Ilastik on the right.

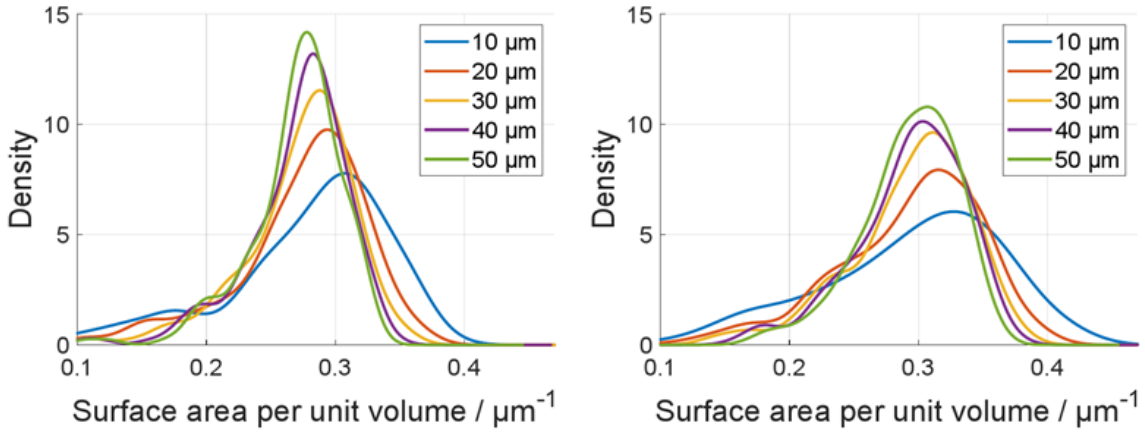

Figure S4. Distribution of the local surface area per unit volume of G-PTMA-CMK-8 (left) and XG-PTMA-CMK-8 (right)

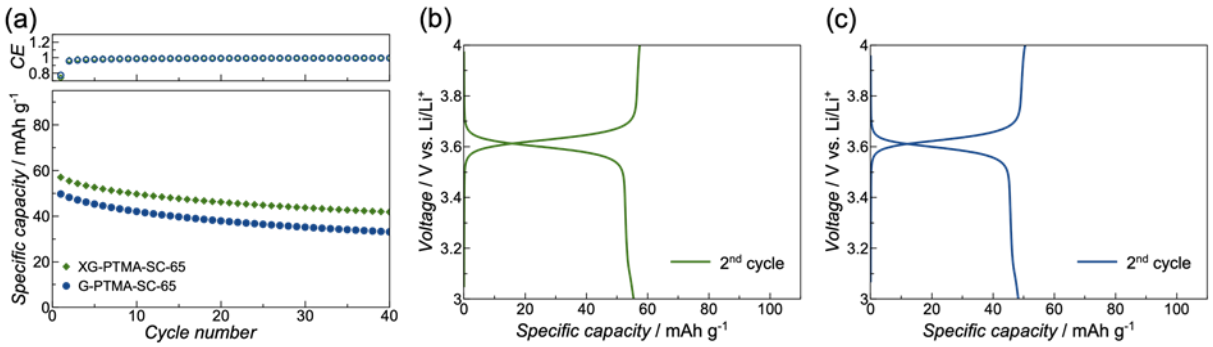

Figure S5. (a) Galvanostatic cycling of XG-PTMA-SC65 (green) and G-PTMA-SC65 electrodes (blue) at a constant specific current of 50 mA g^{-1}. The dis-/charge profile of the 2nd cycle is displayed in panel (b) for XG-PTMA-SC65 and panel (c) for G-PTMA-SC65.

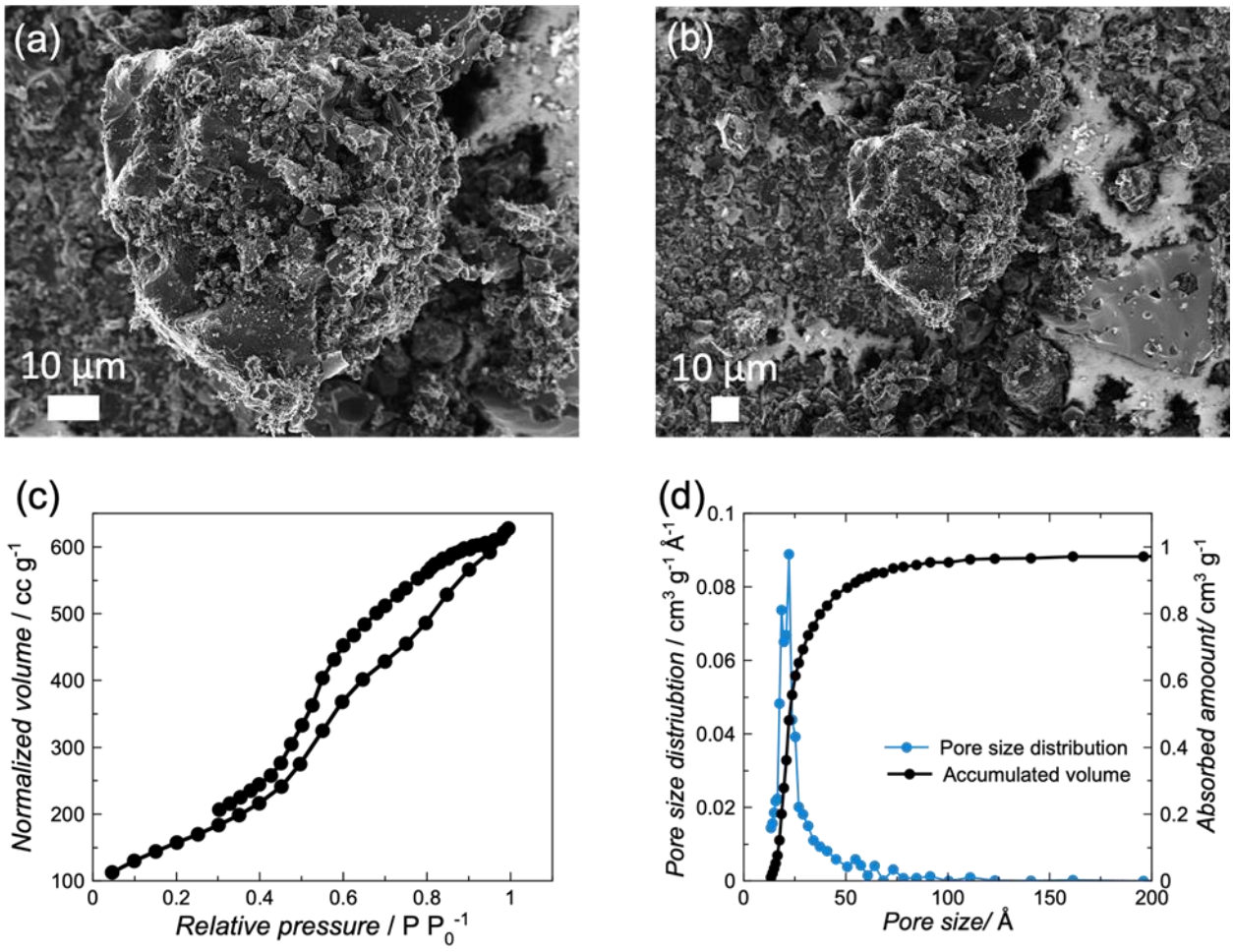

Figure S6. Basic physicochemical characterization of CMK-8 via (a,b) SEM at two different magnifications, (c) BET, and (d) BJH analysis.

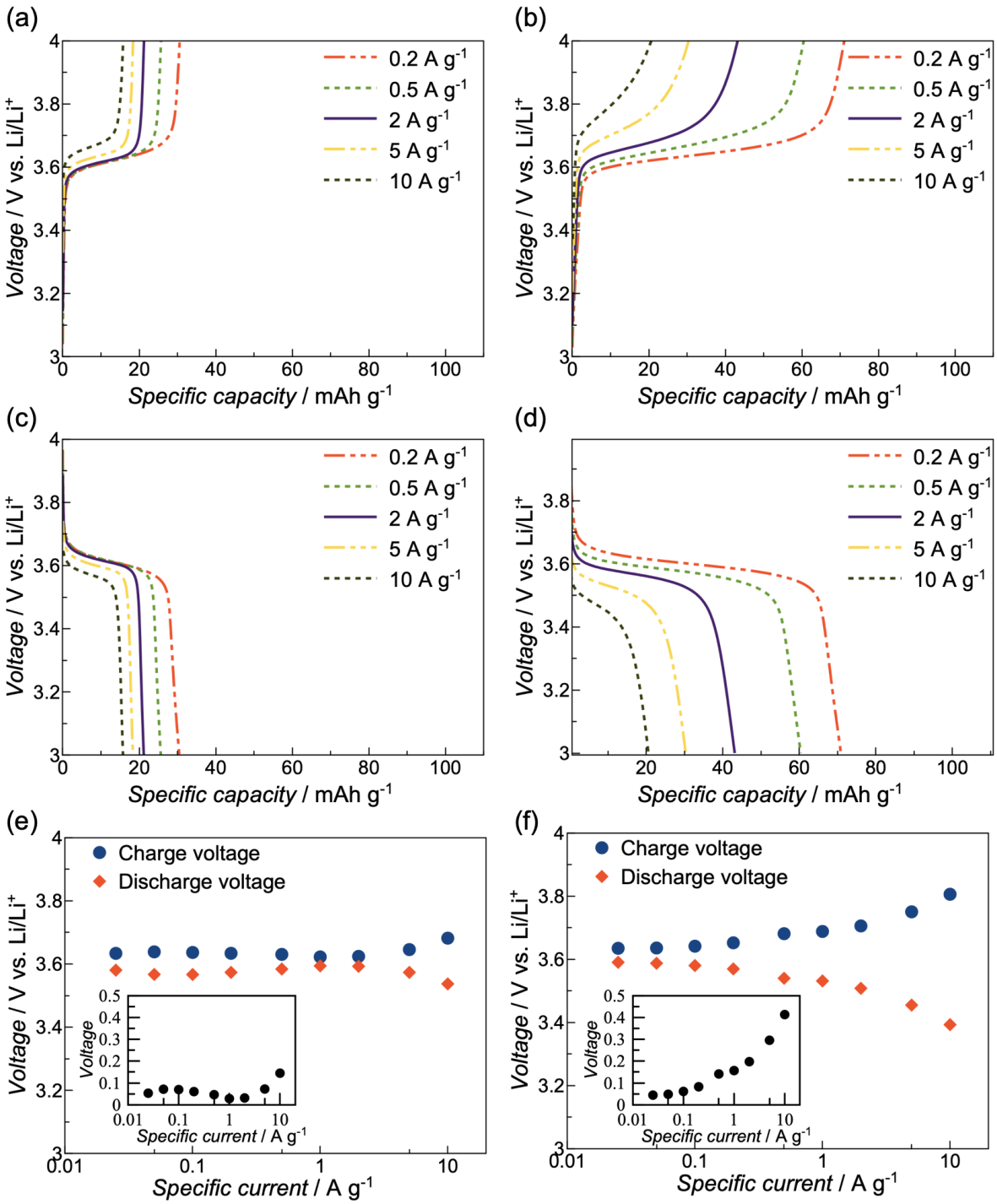

Figure S7. (a,b) Charge and (c,d) discharge profiles of galvanostatically cycled (a,c) G-PTMA-CMK-8 and (b,d) XG-PTMA-CMK-8 electrodes at specific currents varying from 0.2 to 10 A g^{-1}. Plots of the average charge and discharge voltage vs. the applied specific current (logarithmic) for (e) G-PTMA-CMK-8 and (f) XG-PTMA-CMK-8; the inset shows the total dis-/charge hysteresis.